Duta Pharma Journal e-ISSN : 2829-811X, p-ISSN : 2830-7054
Volume 6 Issue 1 June 2026, page 15-30

ATR-FTIR Spectral Profiling and PCA of Red Ginger (*Zingiber officinale* var. rubrum) from Java, Indonesia

Maria Serliati Ngongo, Ellsya Angeline Rawar*, Novena Adi Yuhara
Departement of Pharmacy, Universitas Kristen Immanuel, Yogyakarta, Indonesia
**Corresponding Author*: ellsya@ukrimuniversity.ac.id

Submitted: May 28, 2026 ***Accepted: Juni 15, 2026*** ***Published: Juni 29, 2026***

ABSTRACT

Background: Red ginger (*Zingiber officinale* var. rubrum) is a herbal plant widely used in traditional medicine due to its various bioactive compounds, which are influenced by geographical and agroclimatic conditions. **Objectives**: This study aimed to distinguish the Fourier Transform Infrared (FTIR) spectral profiles of red ginger in Java, Indonesia using Principal Component Analysis (PCA). **Methodology**: Red ginger samples from six regions, namely Jatinangor, Ciamis, Trenggalek, Bogor, Sumedang, and Wonogiri, were dried, ground, and analysed using ATR-FTIR in the wavenumber range of 4000-400 cm^{-1}. The transmittance data were processed using PCA in XLSTAT. Dry weight loss was determined using an oven at 105°C to evaluate the water content of the medicinal plants. **Results**: The results of dry weight loss showed an average value ranging from 9.24% to 11.96%. Samples from Ciamis (11.76%), Sumedang (11.96%), Trenggalek (10.84%), and Bogor (10.15%) exceeded the required standard limit (<10%), while the other samples met the standard requirements. FTIR spectral analysis revealed the presence of O–H, C–H, C=O, C=C, and C–O functional groups associated with gingerol and shogaol compounds. PCA analysis showed that two principal components, PC1 and PC2, explained 96.798% of the total variation in the data. The score plot showed sample clustering by geographical origin, with Jatinangor, Trenggalek, and Bogor exhibiting relatively similar spectral characteristics, whereas Sumedang, Ciamis, and Wonogiri showed distinct profiles. Contribution analysis showed that Ciamis and Wonogiri contributed mostly to the formation of PC1, while Ciamis and Sumedang contributed significantly to PC2. PCA is used to distinguish the spectral profiles of red ginger based on the regional origin of the tested samples as an initial overview for explanation without a validated classification model. **Conclusions**: This study demonstrated that the combination of ATR-FTIR and PCA is an effective, rapid method for differentiating the spectral profiles of red gingers by geographical origin.

Keywords: Red Ginger, Fourier Transform Infrared Spectroscopy, Chemometrics, Principal Component Analysis.

INTRODUCTION

Red ginger (*Zingiber officinale* var. rubrum) is a cultivar of *Zingiber officinale* widely used in Asia, including Indonesia, both as a spice and as an ingredient in traditional medicine (Zhang *et al.*, 2022). The red ginger rhizomes contain various bioactive compounds, including gingerol, shogaol, and zingerone. In addition, they also contain essential oil components that play a role in providing a distinctive aroma and supporting various biological activities (Siregar *et al.*, 2022).

The quality of red ginger can be influenced by various factors, such as its growing region of origin, environmental conditions during growth, and post-harvest stages, including the drying process (Chen *et al*., 2023; Shaukat *et al*., 2024). Differences in these factors can lead to variations in the chemical compound content and physical properties of the herbal medicine (Chen *et al*., 2023; Shaukat *et al*., 2024). Therefore, the capability of an analytical method to comprehensively assess and describe this diversity is needed.

Quality control of herbal raw materials in Indonesia generally still focuses on a single-composite chemical marker approach, such as gingerol or shogaol levels (Li *et al.*, 2008). However, this approach has several limitations, such as the high cost of chemical standards, the relatively complex and time-consuming sample preparation stages, and its inability to represent the synergistic interactions between compounds in multicomponent medicinal plant systems (Balekundri and Mannur, 2020). Therefore, a multicomponent profile-based approach using spectral fingerprint patterns has begun to be widely developed because it is considered more representative in describing the overall chemical complexity of herbal ingredients (Wang and Yu, 2015). One widely used method is Fourier Transform Infrared (FTIR) spectroscopy, known as a chemical fingerprint technique with various advantages, including being fast, non-destructive, efficient, relatively economical, and able to provide comprehensive information on the vibrations of chemical functional groups in samples (Ridho *et al.*, 2019).

Attenuated Total Reflection Fourier Transform Infrared (ATR-FTIR) spectroscopy has been reported to be effective in identifying and differentiating organic components based on their specific molecular bond vibration characteristics. This technique produces an infrared spectrum that represents the overall chemical composition of a sample and can therefore be used as a unique molecular fingerprint to determine product authenticity. In this study, FTIR analysis was only used to observe spectral patterns between red ginger samples from each region of origin, so quantitative analysis of the levels of compounds contained was not carried out.

One method that can be used is multivariate analysis, such as Principal Component Analysis (PCA), which simplifies data dimensions while simultaneously describing relationships between samples based on various observed variables. This method allows for the identification of sample grouping patterns and provides an overview of the contribution of each variable to shaping a sample's characteristics (Amponsah *et al.*, 2022). Fourier Transform Infrared (FTIR) spectroscopy has been combined with chemometrics for rapid and accurate identification and authentication of red ginger (*Zingiber officinale* var. rubrum). The chemometric approach in this system functions to map complex FTIR spectrum data, thus being able to specifically distinguish red ginger from other varieties such as emprit ginger (*Zingiber officinale* var. amarum) and elephant ginger (*Zingiber officinale* var. officinale) (Purwakusumah *et al*., 2014).

Research on red ginger has been conducted in several locations in Indonesia, such as Ciamis, Bogor, Wonogiri, Trenggalek, Sumedang, and Jatinangor (Anjarsari, Umiyati and Murgayanti, 2024; Nana *et al.*, 2021). The selection of Ciamis, Bogor, Wonogiri, Trenggalek, and Sumedang Regencies (including the Jatinangor area) as sampling locations for red ginger was based on the extreme variations in regional physical characteristics, topography, and soil types to analyse the influence of environmental factors on the shelf life or secondary metabolite content of this biopharmaceutical plant. According to its optimal growing requirements, the red ginger plant requires an ideal altitude ranging between 300 and 900 meters above sea level (masl) with fertile soil conditions and proper drainage (Suharno & Heriyanto, 2018). These five selected regions represent highly contrasting ecological gradients; ranging from the Bogor region, which exhibits the most extreme altitude fluctuations from lowlands to cold-climate high mountains (Pemerintah Kabupaten Bogor, 2016), the Ciamis area, which slopes fertility from the north to the southern coast (Badan Pusat Statistik Kabupaten Ciamis, 2024), the Jatinangor volcanic highland basin in Sumedang (Pemerintah Kabupaten Sumedang, 2018), the rugged mountainous terrain in Trenggalek (Badan Pusat Statistik Kabupaten Trenggalek, 2024), to the lowlands dominated by relatively dry karst hills or limestone mountains in Wonogiri (Badan Pusat Statistik Kabupaten Wonogiri, 2024). The striking differences in these abiotic components—such as altitude, limestone versus volcanic soil structures, humidity, and local temperatures of each sampling location—serve as crucial parameters to evaluate the physical adaptability as well as the variability of essential oil content and bioactive compounds (such as gingerol and shogaol) in the resulting red ginger rhizomes. Therefore, the selection of these sampling locations is expected to illustrate the variation in the spectral profile of red ginger related to differences in growing environmental conditions and geographic origin. Each region has unique environmental characteristics that leave a unique "fingerprint" on the chemical profile of plants.

However, an in-depth study that maps the internal variations of the spectral profile of red ginger between specific regions in Java, Indonesia still requires more comprehensive exploration. This study aims to use the combination of ATR-FTIR spectroscopy and PCA in exploring the differences in the spectral profiles of red ginger based on its geographical origin in Java, Indonesia.

MATERIALS AND METHOD

Materials

The materials used in this study were red ginger rhizomes purchased directly from local farmers in Jatinangor, Sumedang, Wonogiri, Bogor, Ciamis, and Trenggalek. The rhizome of red ginger were harvested at an age of approximately 10–12 months after planting because approximately 8–10 months are at the optimal physiological maturity phase (Utami *et al*., 2022). After harvesting, the rhizomes were washed with water, sliced at a thickness of approximately ± 2–3 mm, then dried in an oven at 50°C until they reached a constant weight. Next, the samples were ground into powder and stored in a desiccator at room temperature to maintain stable water content before analysis using ATR-FTIR.

The materials which have been determined in the Laboratorium Struktur dan Perkembangan Tumbuhan (SPT) of the Faculty of Biology, Gajah Mada University, with number 01072/S.Tb/IV/2026 indicate that the plant is indeed red ginger with the variety *Zingiber officinale* var. rubrum Theilade. The dried and powdered red ginger rhizomes will be tested using the infrared spectroscopy method with an ATR-FTIR instrument to identify the functional groups of compounds in red ginger rhizomes from various regions in Java, Indonesia.

The tools used in this study were ATR-FTIR spectroscopy (Shimadzu IR-Spirit T®), analytical balance (Ohaus®), oven (Memmert®), blender (Miyako®), desiccator, porcelain crucible, 100 mesh sieve, and spatula. The software used for statistical analysis with chemometrics was XLSTAT trial version.

Methods

1. Preparation of simplicia

Red ginger rhizomes were washed to remove dirt, then cut into small pieces and dried. Once dry, the samples were blended into powder and sieved using a 100-mesh sieve to obtain uniform particle size before analysis (Rafi *et al*., 2018; Vardana *et al*., 2021).

2. Testing of specific parameters of simple drugs (Organoleptic)

Organoleptic tests included appearance, odour, taste, and colour. Statements such as "odourless," "practically odourless," "slight characteristic odour," or other statements were determined by observing the material after it had been exposed to air for 15 minutes. The 15 minutes was calculated after the container containing no more than 25 g of material was opened and transferred to a 100 mL evaporator dish. Three replicates were performed. (Depkes RI, 2017).

3. Testing of non-specific parameters of simple substances (Drying shrinkage test)

One gram of the simplicia was placed in a shallow, capped weighing bottle that had been previously heated and tared. The material in the bottle was evenly distributed by shaking it to form a layer approximately 5 to 10 mm thick. The bottle was placed in a drying chamber, the cap removed, and dried at a set temperature until a constant weight was reached. Before each drying session, the bottle was left closed to cool in a desiccator to room temperature. Three replicates were performed. (Depkes RI, 2017). Calculation of drying loss using the formula (Depkes RI, 2017) :

$$\%\ Loss\ on\ Drying = \frac{Initial\ Weight\ of\ Simplicia - Final\ Weight\ of\ Simplicia}{Initial\ Weight\ of\ Simplicia}\ x\ 100\%$$

4. Attenuated Total Reflection Fourier Transform Infrared (ATR-FTIR) Spectroscopy Testing

Fourier Transform Infrared Spectroscopy (FTIR) analysis begins with the placement of the sample in a measurement chamber, with three replicate samples from each region using ATR-FTIR parameters (resolution of 2 cm^{-1}, 20 scans per measurement, transmittance mode). The advantage of using an attenuated total reflectance (ATR) accessory is that the analysis can be carried out without complicated sample preparation. (Ridho *et al.*, 2019). Next, the instrument is operated so that the infrared radiation source emits light that is directed toward the Michelson interferometer to produce an interferogram through a process of splitting and combining light beams. (Ni *et al.*, 2020).

The resulting interferogram then interacts with the sample, resulting in absorption of radiation at certain wavenumbers that correspond to the vibrations of functional groups in the molecule. (Hashimoto *et al.*, 2019). The transmitted signal is then captured by a detector and converted into an electrical signal, which is then processed by a computer system using a Fourier transform to produce an infrared spectrum (Nandiyanto *et al.*, 2019). The resulting spectrum is then analysed qualitatively based on characteristic absorption peaks to identify the functional groups present in the sample. In the post-run analysis, a threshold value of 100 and a noise level of 0 are used to obtain optimal spectrum quality, and the main reason for selecting the wavenumber range of 400-4000 is that this range is the mid-infrared (MIR) region. In the world of natural product analysis, this region is the most crucial area because it stores complete structural information about the functional groups of chemical compounds. In the range of 1500-400, there is an area called the fingerprint region. The range of 4000-1500 (functional group region) detects characteristic stretching vibrations of the main secondary metabolites in red ginger (such as gingerol, shogaol, and essential oils).

Data Analysis

The analysis of the FTIR spectrum data of red ginger was carried out through several main stages, including data pre-treatment (preprocessing), principal component analysis (PCA), and interpretation of plots to determine the separating functional groups (Zahara *et al.*, 2023). Before multivariate statistical analysis, data preprocessing involves transforming the raw FTIR spectrum data into transmittance values in specific wavenumber regions, generally in the fingerprint region and the entire mid-IR region 4000-400 cm^{-1} (Rohman *et al.*, 2019). To minimise background noise (baseline shift), sample thickness variations, and instrument noise, spectral data undergo digital pretreatment. Commonly used methods include Standard Normal Variate (SNV) correction (Nandiyanto *et al.*, 2019). This pretreatment is crucial to sharpen the overlapping absorption peaks so that the chemical variations between regions can be optimally extracted (Mallet and Marini, 2022).

In Principal Component Analysis (PCA), the corrected spectrum data were then analysed using an unsupervised pattern recognition method, namely PCA, with the help of chemometrics software. (Triyasmono *et al.*, 2021). Large multivariate data matrices are reduced in dimension into several new orthogonal factors or principal components (PC) (Wulandari, Retnaningtyas and Lukman, 2016). Evaluation of the feasibility of the PCA model is determined based on the eigenvalue and the cumulative variance percentage value (cumulative variance %) which ideally should extract more than 70% to 80% of the total variance of the original data (Biancolillo and Marini, 2018).

Proximity and separation between red ginger samples were evaluated visually through a two-dimensional (2D) observation score plot, usually plotting PC1 against PC2. Coordinate points of red ginger samples that are close to each other show similar spectral profiles (similarity in chemical composition), while samples that are separated into different quadrants show significant chemical variations that are influenced by the geographical origin of the place of growth (Nurmansyah, 2026). Contribution analysis is carried out using loading plots or contribution tables to determine the functional groups and metabolite compounds that play the most role in separating geographic clusters of samples. (Rohman *et al.*, 2021). The wave numbers that have the largest contribution value to PC1 and PC2 are identified (Sukweenadhi *et al.*, 2023).

RESULT AND DISCUSSION

Testing of specific parameters (Organoleptic)

Organoleptic testing is conducted with the aim of initial physical recognition using the three senses to describe the aroma, form, and colour of the simplicia (Kemenkes, 2000). The results of the organoleptic test are showed in Table 1.

Table 1. Organoleptic test of red ginger powder

Sample	Aroma	Form	Colour	Picture
Red Ginger Powder from Jatinangor	Ginger Specialty	Fine Powder	Brownish Yellow	
Red Ginger Powder from Bogor	Ginger Specialty	Fine Powder	Brownish Yellow	
Red Ginger Powder from Sumedang	Ginger Specialty	Fine Powder	Brown	
Red Ginger Powder from Wonogiri	Ginger Specialty	Fine Powder	Brown	
Red Ginger Powder from Ciamis	Ginger Specialty	Fine Powder	Brown	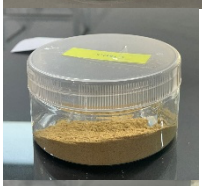
Red Ginger Powder from Tranggalek	Ginger Specialty	Fine Powder	Brownish Yellow	

Non-specific parameter testing (Drying shrinkage)

Table 2. Results of drying shrinkage test (gravimetry)

Sample	Average
Red Ginger from Jatinangor	9.24%
Red Ginger from Ciamis	11.76%
Red Ginger from Tranggalek	10.84%
Red Ginger from Bogor	10.15%
Red Ginger from Sumedang	11.96%
Red Ginger from Wonogiri	9.85%

The drying loss parameter is a measurement of the remaining substance after drying at a temperature of 105 °C until constant weight is expressed as a percentage value of loss on drying (LOD). Knowing the drying loss can provide a maximum limit on the amount of compound lost during the drying process (Kemenkes, 2000). The results of the drying loss test are showed in Table 2.

The results of the drying loss analysis show that the average value for red ginger ranging from 9.24% to 11.96%. Samples from Ciamis (11.76%), Sumedang (11.96%), Trenggalek (10.84%), and Bogor (10.15%) exceeded the required standard limit (<10%), while the other samples met the standard requirements. The moisture content of red ginger (*Zingiber officinale* var. *rubrum*) harvested from different geographical regions, including Ciamis, Sumedang, Trenggalek, and Bogor, exhibited notable variations, with all samples exceeding the 10% threshold. These variations are highly influenced by the distinct agroclimatic conditions of each cultivation site, particularly rainfall patterns and light intensity. Higher rainfall and elevated soil moisture in regions like Bogor and Ciamis naturally increase water accumulation within the rhizome tissue during the vegetative phase. Furthermore, lower light intensity caused by frequent cloud cover or intercropping shading reduces the transpiration rate of the plants, leading to a higher retention of water in the rhizomes. These environmental factors ultimately contribute to the high initial moisture content, which demands more prolonged and strictly controlled post-harvest drying processes to meet standard pharmaceutical requirements (Hayani, 2020).

Data analysis

The FTIR spectra of red ginger from various regions were analysed using the Principal Component Analysis (PCA) method with the help of XLSTAT software. The PCA analysis aims to determine the grouping pattern of samples based on the similarity of FTIR spectrum characteristics and to observe the relationship between red ginger samples from various regions. The results of the PCA analysis are presented in the form of scree plots, biplot, and the contribution of observations.

FTIR spectrum readings were performed sequentially from high to low wavenumbers in the range of 4000-400 cm^{-1}. The vertical axis (y) represents the percentage transmittance (%T), where peaks pointing downwards indicate strong absorbance by specific functional groups. The analysis stages in red ginger begin with sample preparation, followed by spectrum recording, and finally, identification of characteristic peaks to detect active compounds such as gingerols and shogaols based on their functional group vibrations. The absorption peaks of the active compound gingerol include the stretching vibrations of the hydroxyl group (O-H) of the phenolic alcohol group at wave numbers of 3400-3300 cm^{-1}, the stretching vibrations of the aliphatic C-H (-CH_2 and -CH_3) at wave numbers of around 2850 cm^{-1} and 2930 cm^{-1}, the stretching vibrations of the carbonyl group (C=O) in the aliphatic ketone chain at wave numbers of around 1710 cm^{-1} or 1640 cm^{-1}, the stretching vibrations of the C-O in the ether and alcohol groups at wave numbers of 1200-1000 cm^{-1}(Viswanathan, 2018). At the absorption peak of the active compound shogaol, the hydroxyl functional group (-OH) was detected in the wave number range of 3900-3300 cm^{-1} and 1500-400 $cm^{-1,}$ the C-H functional group at wave numbers of 3000-2800 cm^{-1}, the C=O functional group at wave numbers of 1855-1648 cm^{-1}, the C=C functional group at wave numbers of 1680-1400 cm^{-1}, and the C-O functional group at wave numbers of 1300-1000 cm^{-1} and 1500-400 cm^{-1} (Ghorbani and Zargaran, 2024).

Based on Figure 1, there are similarities between the FTIR spectra of red ginger originating from the Jatinangor and Trenggalek areas because there is no peak in the wavenumber region of 2800-3000 cm^{-1}. The FTIR spectra of red ginger originating from Ciamis, Bogor, Sumedang, and Wonogiri are similar because there are some peaks in the wavenumber region of 2800-3000 cm^{-1} and some peaks at a wavenumber of 3000-3500 cm^{-1} with relatively the same shape and intensity.

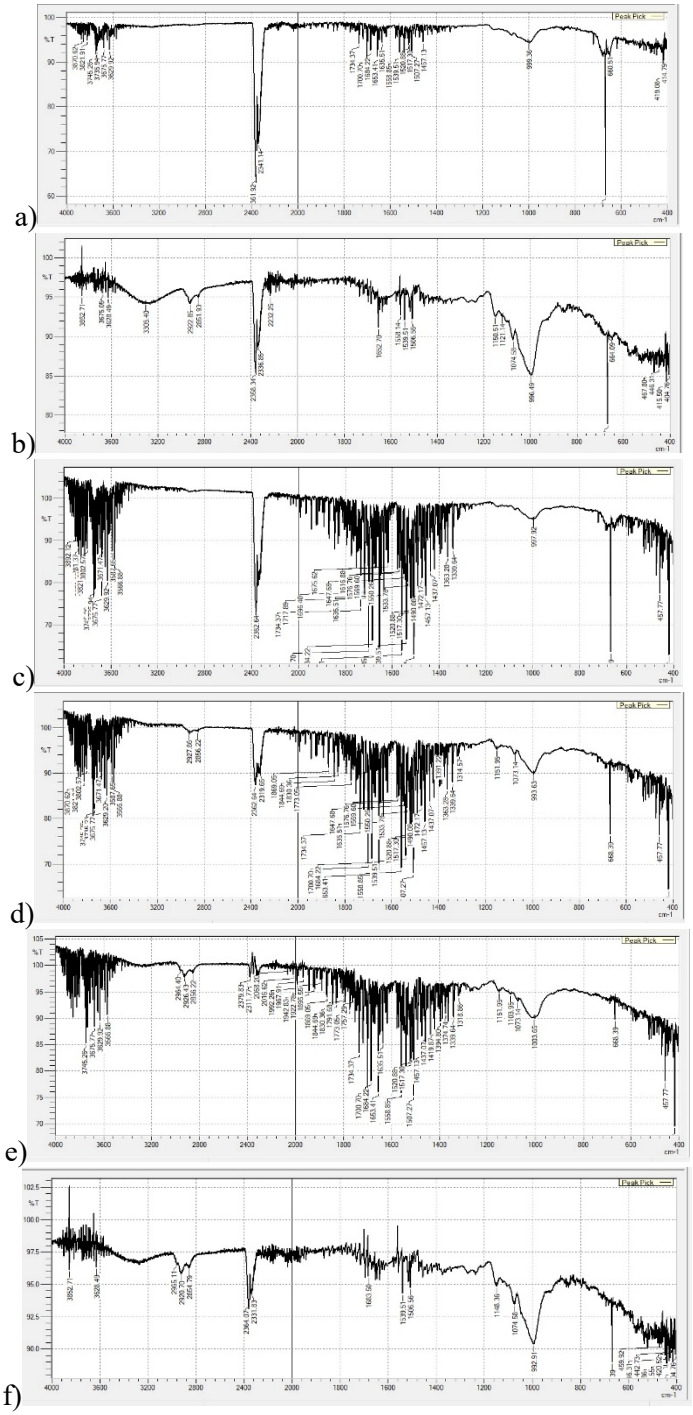

Figure 1. FTIR spectra of red ginger from various geographical origins: a) Jatinangor, b) Ciamis, c) Trenggalek, d) Bogor, e) Sumedang, f) Wonogiri

Table 3. FTIR Spectra Interpretation Results

Wave number	Functional groups	Minimum (T%)	Maximum (T%)	Mean (T%)	Standard deviation
400-667	The fingerprint region is very low, often consisting of vibrations of the carbon skeleton or metal-oxygen/halide bonds.	76-86	90-98	90,930	2,014-4,733
668	C-H out-of-plane bending (alkenes/aromatics)	49,67	85,93	64,472	11,201
669	C-H out-of-plane bending (alkenes/aromatics)	65,73	88,08	76,229	6,632
670-999	C-H out-of-plane bending (alkenes/aromatics)	78-81	93-98	94,291	2,004-4,537
1000-1054	C-O stretching (Alcohol, Ether, Ester) or C-N stretching	78-85	95-96	90,994	3,034-4,489
1055-1158	C-O stretching / C-O-C stretching	85-90	96-97	93,858	2,003-3,069
1506-1560	C=C aromatic ring stretching or N-O stretching (nitro group)	82-86	95-98	91,498	2,247-3,467
1652-1734	C=O stretching (Carbonyl: Amide, Ketone, Aldehyde, Ester, or Carboxylic Acid)	84-89	94-98	92,847	2,224-2,776
2298-2353	O=C=O stretching (Carbon dioxide)	62-88	94-96	81,542	2,001-9,740
2354-2381	O=C=O stretching (environmental CO_2)	52-87	93-95	76,382	2,273-12,705
3629-3854	O-H stretching (free alcohol/phenol) or water vapour (H_2O)	87-92	96-101	94,454	2,161-2,388

Note : T% = percentation of transmittance

The functional group characterisation of the sample was carried out using Fourier Transform Infrared (FTIR) spectroscopy in the wavenumber range of 4000–400 cm^{-1} to identify the main chemical bonds and metabolites contained there. Based on the spectrum profile obtained (Table 3), the area below the wavenumber of 1500 cm^{-1} is dominated by a very specific fingerprint region. At very low transmittance in the range of 400–667 cm^{-1}, the presence of carbon skeleton vibrations was detected, as well as possible contributions from metal-oxygen bonds or inherent halides of the sample (Nakamoto, 2009). Confirmation of the presence of unsaturated hydrocarbon compounds and cyclic structures is strengthened by the appearance of sharp peaks at wavenumbers of 668 cm^{-1} and 669 cm^{-1}, as well as in the range of 670–999 cm^{-1}, which consistently correspond to out-of-plane bending vibrations of the cm^{-1} bonds in the alkene group and aromatic ring (Silverstein *et al*., 2014).

Furthermore, significant absorption intensities in the wavenumber ranges of 1000–1054 cm^{-1} and 1055–1158 cm^{-1} indicate the presence of single-bond stretching vibrations C-O, as well as stretching vibrations C-O-C. The presence of these groups is generally a strong marker for carbohydrate macromolecules, glycoside compounds, or ester alcohol groups associated with phenolic compounds and flavonoids. The aromatic core structure was definitively confirmed through the appearance of peaks in the range of 1506–1560 cm^{-1} originating from aromatic ring stretching, with possible overlapping of nitro groups. Strong characteristics of carbonyl compounds were also identified at wavenumbers 1652–1734 cm^{-1}, which refer to carbonyl bond stretching. The flexibility of this range indicates the presence of various carbonyl functionalities, such as amide groups, ketones, aldehydes, esters, or free carboxylic acids (Barth, 2007).

On the other hand, the spectra also recorded several functional peaks at higher wavenumbers. The appearance of peaks in the ranges of 2298–2353 cm^{-1} and 2354–2381 cm^{-1} theoretically corresponds to the asymmetric stretching of carbon dioxide molecules (O=C=O stretching). The presence of these peaks most likely represents residual CO_2 gas from the ambient atmosphere surrounding the sample chamber during the measurement or may also indicate the presence of traces of alkyne or nitrile groups if supported by other chemical characterisations. Finally, absorption in the high wavenumber range of 3629–3854 cm^{-1} confirmed the presence of free hydroxyl group stretching vibrations (O–H stretching). The sharp peak pattern in this area indicates the presence of phenol or alcohol groups that are not strongly bound by intermolecular hydrogen bonds, or a minor contribution from residual water vapour (H_2O) in the sample matrix (Pavia *et al*., 2015). Overall, this integrative combination of phenolic, aromatic, carbonyl, and carbohydrate functional groups confirm the abundance of the target bioactive compounds in the studied samples.

Eigenvalue Analysis Results

A vector is defined as a quantity that has both a value (magnitude) and a direction. In linear algebra, an eigenvector is a special vector that exhibits unique characteristics when multiplied by a matrix. The resulting vector remains in the same direction but changes in length based on a scaling factor called the eigenvalue. When this concept is applied to Principal Component Analysis (PCA) for FTIR spectral analysis, the eigenvalues of the covariance or correlation matrix represent the degree of variability in the spectral data across each dimension. A large eigenvalue indicates significant variation in the data along the corresponding eigenvector direction, while a small value indicates minimal variation. Therefore, eigenvalues play a crucial role in FTIR spectral similarity analysis; the higher the value, the greater the contribution of the variable or principal component in determining spectral similarity, ultimately improving the accuracy of identifying characteristic sample patterns.

Table 4. Results of eigenvalue analysis of FTIR spectra of red ginger

Principal Component	Eigenvalue	Variability (%)	Cumulative (%)
F1 (PC1)	16147.768	76.052	76.052
F2 (PC2)	4404.827	20.746	96.798
F3 (PC3)	317.521	1.495	98.293
F4 (PC4)	124.040	0.584	98.877
F5 (PC5)	61.346	0.289	99.166
F6 (PC6)	54.775	0.258	99.424
F7 (PC7)	34.084	0.161	99.585
F8 (PC8)	20.253	0.095	99.680
F9 (PC9)	12.602	0.059	99.739
F10 (PC10)	10.094	0.048	99.787
F11 (PC11)	8.454	0.040	99.827
F12 (PC12)	7.594	0.036	99.863
F13 (PC13)	7.112	0.033	99.896
F14 (PC14)	6.603	0.031	99.927
F15 (PC15)	5.860	0.028	99.955
F16 (PC16)	5.076	0.024	99.979
F17 (PC17)	4.541	0.021	100.000

Table 4 presents the results of the eigenvalue analysis and the variance contribution of the FTIR spectrum of red ginger, reduced using Principal Component Analysis (PCA). This multivariate analysis successfully extracted 17 factors or principal components (PC1 to PC17) from the original dataset. In chemometrics, the eigenvalue reflects the amount of variance or total information that can

be explained by each factor. Based on the data obtained, the eigenvalue decreases significantly from the first to the last factor. Factor 1 (PC1) has the largest eigenvalue of 16147.768, followed by Factor 2 (PC2) at 4404.827. After the second factor, the eigenvalue decreases drastically below 318 in Factor 3 (F3) and continues to decrease until Factor 17 (PC17) is only 4.541. To determine the most optimal and representative number of principal components in modelling red ginger samples, the main references used were the percentage values of individual variability (Variability %) and cumulative (Cumulative %). The first factor (PC1) was able to explain a very dominant data variability, namely 76.052%, while the second factor (PC2) was able to explain the variability of 20.746%. When these two factors were combined, the resulting cumulative variance value reached 96.798%. In chemometric analysis, a PCA model is considered very strong and representative if the cumulative variance value of the selected principal components has exceeded the threshold of 70% to 80%. Because the combination of PC1 and PC2 alone was able to capture almost all of the total data variability (96.798%), factors F3 to PC17 can be ignored in further analysis because they only contain very small residual variance, which is most likely noise or background interference from the instrument.

The high variability values captured by PC1 and PC2 have a chemical meaning that is closely related to the spectral characteristics of red ginger. This indicates a strong pattern of chemical differences or functional group absorbance between the tested red ginger samples, which can be influenced by variations in growing location, harvest age, and extraction method. In this context, PC1 with a percentage of 76.052% most likely represents variations in the main or majority chemical components contained in red ginger. Meanwhile, PC2 with a percentage of 20.746% is strongly suspected to distinguish the more fluctuating secondary metabolites typical of red ginger. Thus, the visualisation of complex red ginger FTIR spectra data can be simplified by using a two-dimensional score plot based on PC1 and PC2, because this model is very valid in representing all the chemical information of the sample without eliminating essential data.

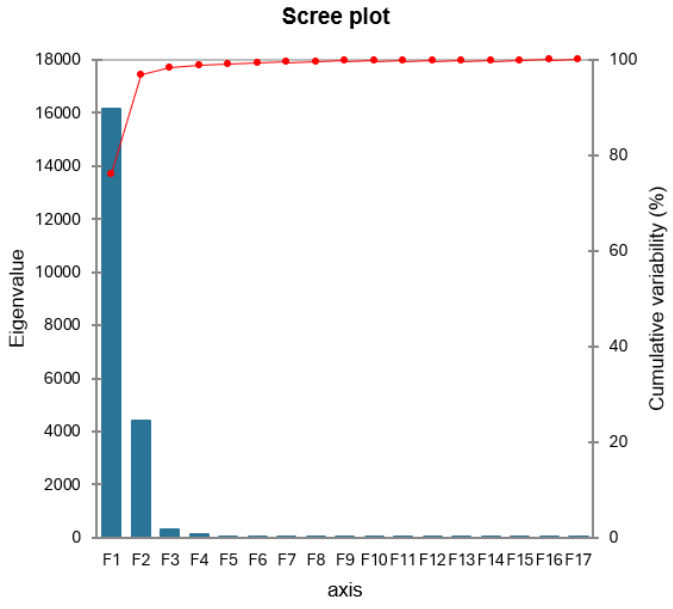

Figure 2. Scree plot of the FTIR spectra of red ginger from different geographical origins

Figure 2 presents a scree plot graph, which is a visual representation of the results of the eigenvalue analysis and the cumulative variance of the FTIR spectra of red ginger from various regions. This graph is very useful in principal component analysis (PCA) to help determine the optimal number of factors in reducing the dimensionality of the data without losing essential information. The blue bars in the graph depict the eigenvalues for each factor (axis PC1 (F1) to PC17 (F17)) on the left y-axis, while the red line with the marker points shows the percentage of cumulative

variability (Cumulative variability %) on the right y-axis. Visually, the shape of the curve in the graph shows a very sharp decline (sharp elbow) from Factor 1 (PC1) to Factor 2 (PC2), and a drastic slope starting from Factor 3 (PC3) to Factor 17 (PC17). The change in slope that forms a sharp "elbow" clearly confirms that the variation in the red ginger spectral data is predominantly centred on the first two principal components only (Rafi *et al.*, 2021).

From an analytical chemistry perspective, the successful clustering of dominant variances on PC1 and PC2 in this scree plot reflects the big differences in metabolite profiles in red ginger samples due to geographic influences or their growing regions of origin. Differences in soil, climate, elevation, and nutrient conditions across these regions of origin are well recorded in the shifts or absorption intensities of specific functional groups in the FTIR spectra, which are then optimally extracted by PC1 and PC2. Therefore, this scree plot graph provides a strong theoretical basis for limiting principal component analysis to a two-dimensional model (2D score plot). This data reduction approach has proven to be very valid and efficient for differentiating or grouping red ginger based on its region of origin (Jolliffe and Cadima, 2016).

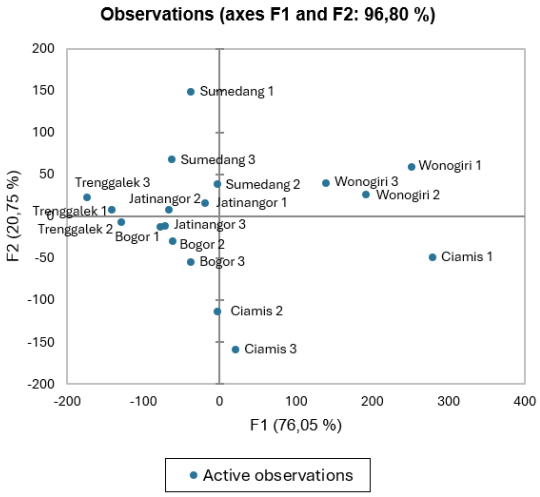

Figure 3. Observation plot of FTIR spectra of red ginger from various regions

Figure 3 displays a two-dimensional observation score plot with axes F1 (PC1) and F2(PC2) based observation score plot that clarifies the clustering of red ginger samples based on their region of origin. Through the distribution of coordinate points on this score plot, it is clearly visible that red ginger samples from the same region tend to be close together or clustered in the same quadrant. This phenomenon proves that the combined method of FTIR spectroscopy and principal component analysis (PCA) has very strong discrimination and classification capabilities in objectively identifying the geographic identity or fingerprint of red ginger commodities.

Based on the proximity between coordinate points on the graph, the red ginger samples are consistently separated into several main clusters along the horizontal (PC1) and vertical (PC2) axes. In the right area (positive PC1 values), a very clear cluster is formed for the Wonogiri sample group (Wonogiri 1, 2, and 3) in the upper right quadrant, and the Ciamis samples (Ciamis 1, 2, and 3) spread across the lower area (negative PC2 values). The separation of the Wonogiri and Ciamis groups along the positive PC1 axis indicates a similarity in the chemical content profiles or absorption intensity of certain functional groups that are dominant in both areas compared to other areas. On the other hand, the Sumedang samples (Sumedang 1, 2, and 3) cluster vertically around the upper central axis (positive PC2 values), indicating specific secondary metabolite characteristics that distinguish them from other groups.

Meanwhile, in the left area of the graph (negative PC1 value), there is a fairly intense spatial overlap between the sample groups from Jatinangor, Bogor, and Trenggalek. The Jatinangor (1, 2, 3) and Bogor (1, 2, 3) samples overlap each other around the lower left quadrant, followed by the Trenggalek samples (1, 2, 3), which are slightly shifted to the extreme left. This positional closeness

phenomenon reflects that red ginger from the Jatinangor, Bogor, and Trenggalek areas has very similar FTIR spectral profiles, which means that the composition of the majority and minority chemical compounds in these samples is relatively uniform. Overall, the clear separation of the Wonogiri, Ciamis, and Sumedang groups, as well as the joint grouping of Jatinangor, Bogor, and Trenggalek, confirms that variations in external environmental factors such as agroclimate, soil type, altitude, and rainfall in each region of origin have successfully influenced the biosynthesis of metabolites in red ginger specifically, so that it can be read well through this PCA modelling (Rohman *et al.*, 2021).

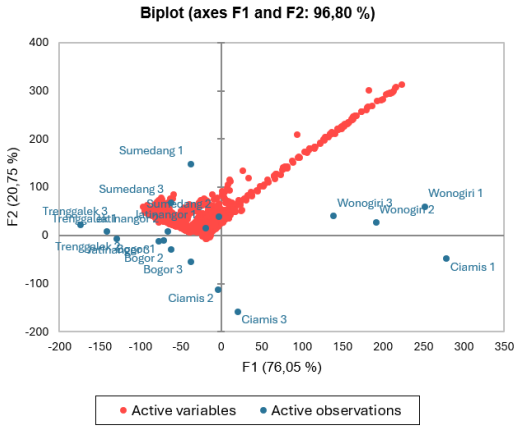

Figure 4. Biplot

Figure 4 represented through the biplot graph in the image above, it can be seen that the visualisation is able to explain the data variability very comprehensively. The distribution pattern of samples or observations in the graph indicates specific groupings based on the geographic region of origin of the samples. The observation clusters from the Wonogiri region (Wonogiri 1, Wonogiri 2, and Wonogiri 3) are strongly concentrated in the right quadrant with a positive F1 (PC1) value. This indicates that samples from these areas have chemical or physicochemical characteristics that are linear and positively correlated with the majority of active variables that spread diagonally to the upper right (Nurmansyah, 2026). On the other hand, samples from the Trenggalek region (Trenggalek 1, Trenggalek 2, Trenggalek 3) and Jatinangor show close euclidean distances in the upper left quadrant, indicating significant profile similarities between the two regional clusters, but have characteristic trends that are in the opposite direction to the Wonogiri sample group.

Meanwhile, quite contrasting internal variability was detected in samples from Ciamis (Ciamis 1, Ciamis 2, and Ciamis 3) and Sumedang. The Ciamis samples were spread vertically along the negative F2 (PC2) axis, with the Ciamis 3 subsample at the lowest F2 ordinate. The scatter pattern of the predominantly elongated active variables triggered strong multicollinearity among the test parameters in the first quadrant. The accumulation of active variables in a single linear corridor indicates that the measured markers simultaneously influence each other, thus differentiating sample clusters. (Nurmansyah, 2026). This difference in spatial distribution emphasises that environmental agroclimatology factors, soil microclimate conditions, and geographic variations play a crucial role in the formation of metabolite profiles or physicochemical parameters of the samples tested in each region.

Table 5 presents data on the relative contribution values (in per cent) of each red ginger sample based on its region of origin to the formation of the main components or factors (PC1 to PC5) in the PCA analysis. This contribution value is crucial in chemometrics because it shows which samples act as the main characteristics (key drivers) or have the greatest influence on the separation formed in the score plot graph. Considering that the previous two-dimensional analysis (PC1 and PC2) has covered 96.80% of the total data variability, the interpretation of this contribution is prioritised on the values contained in the PC1 and PC2 columns to identify the samples most responsible for the separation of the red ginger geographic clusters.

Table 5. Contribution of FTIR spectra from various regions to the observation plot

Region of origin	PC1	PC2	F3	F4	F5
Jatinangor 1	0,125	0,301	11,075	14,662	15,759
Jatinangor 2	1,488	0,083	11,182	12,998	0,006
Jatinangor 3	2,044	0,207	12,368	4,583	4,109
Sumedang 1	0,473	**27,738**	1,025	0,146	13,606
Sumedang 2	0,004	1,883	1,343	18,526	4,194
Sumedang 3	1,330	5,881	0,884	3,577	0,011
Bogor 1	1,733	0,148	0,915	4,822	0,933
Bogor 2	1,294	1,119	0,452	9,471	8,096
Bogor 3	0,489	3,794	2,401	13,831	3,793
Wonogiri 1	**21,829**	4,448	2,552	1,029	0,480
Wonogiri 2	**12,593**	0,877	3,096	0,254	7,370
Wonogiri 3	6,673	2,015	12,339	0,059	7,562
Trenggalek 1	6,832	0,076	5,421	0,164	7,641
Trenggalek 2	5,753	0,057	6,273	0,000	2,183
Trenggalek 3	10,441	0,642	3,947	3,286	3,838
Ciamis 1	**26,749**	2,942	16,052	0,307	17,924
Ciamis 2	0,004	**16,085**	0,761	11,015	0,051
Ciamis 3	0,148	**31,705**	7,914	1,271	2,442

In the Factor 1 (PC1) column, which holds the largest variability (76.05%), samples from the Ciamis 1 and Wonogiri areas provide a very dominant contribution value. Ciamis 1 recorded the highest contribution of 26.749%, followed significantly by Wonogiri 1 (21.829%) and Wonogiri 2 (12.593%), and Trenggalek 3 (10.441%). The high contribution value of these samples explains why, in the previous observation plot graph, the Wonogiri, Ciamis 1, and Trenggalek 3 groups are at the extreme pole positions (rightmost or leftmost positions) along the horizontal axis of PC1. This indicates that the FTIR spectra profiles of the Ciamis 1 and Wonogiri 1 samples have very strong and contrasting functional group absorbance variations, making them the main determinant of the differentiation of red ginger macro-chemical characteristics on the main axis of the PCA. In contrast, samples from Jatinangor, Sumedang, and Bogor contributed very little to PC1 (the majority < 2%), which explains why these sample groups are closely clustered in the central area of the graph near the vertical axis.

Meanwhile, in the Factor 2 (PC2) column, which represents 20.75% variability, the contribution map experienced a significant shift towards samples from Ciamis and Sumedang. The Ciamis 3 sample provided the largest contribution on this axis, reaching 31.705%, followed by Sumedang 1 at 27.738%, and Ciamis 2 at 16.085%. The massive contribution figures from Ciamis 3, Ciamis 2, and Sumedang 1 on PC2 underlie the wide vertical distribution of these samples on the score plot. The characteristic of high fluctuations in contribution values on PC2 is strongly suspected to be related to differences in the levels of specific secondary metabolite components which are very sensitive to local agroclimatic influences in Ciamis and Sumedang. Overall, the contribution data in Table 5 provides valid mathematical justification that the separation of red ginger clusters in the observation plot did not occur randomly, but was strongly driven by the Ciamis and Wonogiri samples on the PC1 axis, and the Ciamis and Sumedang samples on the PC2 axis (Nurmansyah, 2026).

By analysing these spectral variations using ATR-FTIR combined with Principal Component Analysis (PCA), samples can be differentiated and grouped according to their geographical origin. Therefore, this approach has the potential to support the geographical origin traceability of red ginger based on its spectral profile. However, this research is still qualitative in nature, so it cannot determine

the absolute levels of bioactive compounds, and the results of the analysis can be influenced by differences in water content in post-harvest samples.

CONCLUSION

The combination of ATR-FTIR spectroscopy and PCA shows potential for distinguishing the spectral profiles of red ginger based on the regional origin of the tested samples. Eigenvalue analysis and scree plots demonstrated robust 2D models (PC1 and PC2) explaining 96.798% of the total data variability. The score plot showed that Wonogiri and Ciamis, and Sumedang samples were clearly separated into independent clusters, while Jatinangor, Bogor, and Trenggalek clustered closely due to their similar chemical profiles. This clustering was mathematically driven by the strong contributions of Ciamis and Wonogiri samples to PC1, and Ciamis and Sumedang to PC2. However, this interpretation is still preliminary due to the limited sample size. Further research with a larger sample size and external validation is needed to strengthen the accuracy of this classification model.

REFERENCES

Amponsah, I.K., Boakye, A., Orman, E., Armah, F.A., Boarquaye, L.S., Adjei, S., Dwamena, Y.A., Baah, K.A., Harley, B.K. (2022) 'Assessment of some quality parameters and chemometric-assisted FTIR spectral analysis of commercial powdered ginger products on the Ghanaian market', *Heliyon*, 8(2022), pp. e09150. Available at: https://doi.org/10.1016/j.heliyon.2022.e09150

Anjarsari, I.R.D., Umiyati, U. and Murgayanti (2024) 'Optimasi Budidaya Jahe Merah: Strategi Pengembangan untuk Meningkatkan Produksi dan Kualitas di Desa Pasigaran Kecamatan Tanjungsari Kabupaten Sumedang', *Jurnal Aplikasi Ipteks untuk Masyarakat*, 13(4), pp. 282–289. Available at: https://jurnal.unpad.ac.id/dharmakarya/article/view/57684

Badan Pusat Statistik Kabupaten Ciamis. (2024). Kabupaten Ciamis Dalam Angka 2024. BPS Kabupaten Ciamis.

Badan Pusat Statistik Kabupaten Trenggalek. (2024). Kabupaten Trenggalek Dalam Angka 2024. BPS Kabupaten Trenggalek.

Badan Pusat Statistik Kabupaten Wonogiri. (2024). Kabupaten Wonogiri Dalam Angka 2024. BPS Kabupaten Wonogiri.

Balekundri, A. and Mannur, V. (2020) 'Quality control of the traditional herbs and herbal products : a review', *Future Journal of Pharmaceutical Sciences*, 6(67), pp. 1–9. Available at: https://doi.org/https://doi.org/10.1186/s43094-020-00091-5

Barth, A. (2007). 'Infrared spectroscopy of proteins', *Biochimica et Biophysica Acta (BBA)-Bioenergetics*, 1767(9), pp. 1073–1101. Available at: https://www.sciencedirect.com/science/article/pii/S0005272807001375

Biancolillo, A. and Marini, F. (2018) 'Chemometric Methods for Spectroscopy-Based Pharmaceutical Analysis', *Frontiers in Chemistry*, 6(November), pp. 1–14. Available at: https://doi.org/10.3389/fchem.2018.00576.

Chen, K., Yuan, Y., Zhao, B., Kaveh, M., Beigi, M., Zheng, Y., & Torki, M. (2023) 'Optimum drying conditions for ginger (*Zingiber officinale* Roscoe) based on time, energy consumption and physicochemical quality', *Food Chemistry: X*, *20*, 100987. Available at: https://doi.org/10.1016/j.fochx.2023.100987

Depkes RI (2017) 'Farmakope Herbal Indonesia Edisi II Tahun 2017'. Jakarta, Indonesia: Departemen Kesehatan Republik Indonesia.

Ghorbani, R. and Zargaran, A. (2024) 'Synthesis and Identification of Shogaol Compounds from the Raw Material Vanillin', *Biological and Molecular Chemistry*, 2(2), pp. 141–151. Available at: https://doi.org/10.22034/bmc.2024.493368.1045

Hashimoto, K. Badarla, V.R., Kawai, A, Ideguchi, T. (2019) 'Complementary vibrational spectroscopy', *Nature Communications*, 10, pp. 1–6. Available at: https://doi.org/10.1038/s41467-019-12442-9.

Hayani, F. (2020). Pengaruh Cekaman Lingkungan Dan Variasi Geografis Terhadap Kadar Air Serta

Profil Fitokimia Simplisia Jahe Merah. Balai Penelitian Tanaman Rempah dan Obat (BALITTRO).

Jolliffe, I.T, Cadima, J., (2016) 'Principal component analysis: a review and recent developments', *Phil. Trans. R. Soc. A*, 374:20150202. Available at: http://dx.doi.org/10.1098/rsta.2015.0202

Li, S. Han, Q., Qiao, C., Song, J., Cheng, C.L., Xu, H. (2008) 'Chemical markers for the quality control of herbal medicines : an overview', *Chinese Medicine*, 3(7), pp. 1–16. Available at: https://doi.org/10.1186/1749-8546-3-7

Nandiyanto, A.B.D., Oktiani, R., Ragadhita, R. (2019) 'How to Read and Interpret FTIR Spectroscope of Organic Material', *Indonesian Journal of Science & Technology*, 4(1), pp. 97–118. Available at: https://doi.org/10.17509/ijost.v4i1.15806

Nakamoto, K. (2009). Infrared and Raman Spectra of Inorganic and Coordination Compounds, Part A: Theory and Applications in Inorganic Chemistry. John Wiley & Sons.

Nana, Makiyah, Y.S., Susanti, E., Ramadhan, I.R., Bhinekas, R.Y., Kanti, L. (2021) 'Budidaya Dan Pengolahan Jahe Merah (*Zingiber officinale* var.rubrum) Menggunakan Teknologi Bag Culture Pada Masa New Normal Di Desa Darmaraja Kecamatan Lumbung Kabupaten Ciamis', *Abdimas Umtas: Jurnal Pengabdian Kepada Masyarakat*, 4(1), pp. 584–593. Available at: https://doi.org/https://doi.org/10.35568/abdimas.v4i1.1038

Ni, Z., Lu., Q., Xu, Y. Huo, H. (2020) 'Intensity Simulation of a Fourier Transform Infrared Spectrometer', *Sensor*, 20 (7), p. 1833. Available at: https://doi.org/doi:10.3390/s20071833

Nurmansyah, A, Shiyan, S., Arina, Y., Sopyan, I., Muchtaridi (2026) 'Chemometric classification of red ginger (*Zingiber officinale* var. rubrum) oleoresin from different regions using Fourier-transform infrared-ATR spectroscopy', *J.Adv.Pharm.Technol.Res*, 17(1), pp. 51–58. Available at: https://doi.org/10.4103/JAPTR.JAPTR_175_25

Pavia, D. L., Lampman, G. M., Kriz, G. S., & Vyvyan, J. A. (2015). Introduction to Spectroscopy (5th ed.). Cengage Learning.

Pemerintah Kabupaten Bogor. (2016). Peraturan Daerah Kabupaten Bogor Nomor 11 Tahun 2016 tentang Rencana Tata Ruang Wilayah Kabupaten Bogor Tahun 2016-2036. Sekretariat Daerah Kabupaten Bogor.

Pemerintah Kabupaten Sumedang. (2018). Peraturan Daerah Kabupaten Sumedang Nomor 4 Tahun 2018 tentang Rencana Tata Ruang Wilayah Kabupaten Sumedang Tahun 2018-2038. Sekretariat Daerah Kabupaten Sumedang.

Purwakusumah, E.D., Rafi, M., Syafitri, U.D., Nurcholis, W., Adzkiya, M.A.Z. (2014) 'Identifikasi dan Autentikasi Jahe Merah Menggunakan Kombinasi FTIR dan Kemometrik', *Agritech*, 34 (1), pp. 82-87. https://www.neliti.com/id/publications/90545/identifikasi-dan-autentikasi-jahe-merah-menggunakan-kombinasi-spektroskopi-ftir

Rafi, M., Rismayani, W., Sugiarti, R.M., Syafitri, U.D., Wahyuni, W.T., Rohaeti, E. (2021) 'FTIR-based Fingerprinting Combined with Chemometrics for Discrimination of Sonchus arvensis leaf Extracts and Correlation with Their Antioxidant Activity', *Indonesian Journal of Pharmacy*, 32(2), pp. 132–140. Available at: https://doi.org/10.22146/ijp.755

Ridho, A., Wathoni, N., Subarnas, A., Levita, J. (2019) 'Insights of phytoconstituents and pharmacological activities of Salacca plants', *Journal of Applied Pharmaceutical Science*, 9(10), pp. 120–124. Available at: https://doi.org/10.7324/JAPS.2019.91017

Roger, J., Mallet, A. and Marini, F. (2022) 'Preprocessing NIR Spectra for Aquaphotomics', *Molecules*, 27(20), 6795. Available at: https://doi.org/10.3390/molecules27206795

Rohman, A, Windarsih, A., Hossain, M., Johan, M.R., Ali, M.E., Fadzilah, N.A. (2019) 'Application of near- and mid-infrared spectroscopy combined with chemometrics for discrimination and authentication of herbal products : A review', *Journal of Applied Pharmaceutical Science*, 9(03), pp. 137–147. Available at: https://doi.org/10.7324/JAPS.2019.90319

Rohman, A., Luthfianasari, H., Irnawati, Riyanto, S., Rafi, M., Prajogo, B., Amran, M.B. (2021) 'HPLC-FTIR spectroscopy combined with multivariate calibration for analysis of Andrographolide in Andrographis paniculata extract', *Journal of Applied Pharmaceutical Science*, 11(05), pp. 32–38. Available at: https://doi.org/10.7324/JAPS.2021.110505

Shaukat, M. N., Fallico, B., & Nazir, A. (2024) 'Impact of air-drying temperatures on drying kinetics,

physicochemical properties, and bioactive profile of ginger', *Foods*, *13*(7), 1096. Available at: https://doi.org/10.3390/foods13071096

Silverstein, R. M., Webster, F. X., Kiemle, D. J., & Bryce, D. L. (2014). Spectrometric Identification of Organic Compounds (8th ed.). John Wiley & Sons.

Siregar, P.N.B., Pedha, K.I.T., Resmianto, K.F.W., Chandra, N., Maharani, V.N., Riswanto, F.D.O. (2022) 'Kandungan Kimia Jahe Merah (*Zingiber officinale* var. rubrum) dan Pembuktian In Silico sebagai Inhibitor SARS-CoV-2', *Jurnal Pharmascience*, 9(2), pp. 185–200. Available at: https://doi.org/http://dx.doi.org/10.20527/jps.v9i2.13149

Stuart, B. H. (2004). Infrared Spectroscopy: Fundamentals and Applications. John Wiley & Sons.

Suharno, & Heriyanto. (2018). Produksi Tanaman Biofarmaka. Pusat Pendidikan Pertanian Badan Penyuluhan dan Pengembangan SDM Pertanian Kementerian Pertanian.

Sukweenadhi, J., Damitasari, P.D., Kartini, Christanti, P., Putri, E.N. (2023) 'Gingerol and shogaol on red ginger rhizome (*Zingiber officinale* var.rubrum) using high-performance liquid chromatography', *Pharmaciana*, 13(2), pp. 166–178. Available at: https://doi.org/10.12928/pharmaciana.v13i2.25246

Triyasmono, L., Munisa, I., Anwar, K., Wianto, T., Santoso, H.B., Rohman, A. (2021) 'Identification and authentication of *Eurycoma longifolia* root extract from *Zingiber officinale* rhizome using FTIR spectroscopy and chemometrics', *Indonesia Journal of Chemometrics and Pharmaceutical Analysis*, 1(2), pp. 69–77. Available at: https://journal.ugm.ac.id/v3/IJCPA/article/view/639

Utami, D.A, Yusraini, E., Ridwansyah, Lubis, Z. (2022) 'Physical characteristics of ginger tuber based on harvesting age and varieties', *IOP Conf. Ser.: Earth Environ. Sci.*, 977 (012078). Available at: https://iopscience.iop.org/article/10.1088/1755-1315/977/1/012078

Viswanathan, K. (2018) 'Effect of nature-based antioxidant from *Zingiber officinale* Rosc. on the oxidation stability, engine performance and emission characteristics with neem oil methyl ester', *Heat and Mass Transfer*, 54, pp 3409-3420. Available at: https://doi.org/10.1007/s00231-018-2380-9

Wang, P. and Yu, Z. (2015) 'Species authentication and geographical origin discrimination of herbal medicines by near infrared spectroscopy : A review', *Journal of Pharmaceutical Analysis*, 5(5), pp. 277–284. Available at: https://doi.org/10.1016/j.jpha.2015.04.001

Wulandari, L., Retnaningtyas, Y. and Lukman, H. (2016) 'Analysis of Flavonoid in Medicinal Plant Extract Using Infrared Spectroscopy and Chemometrics', *Journal of Analytical Methods in Chemistry*, 1, pp. 1–6. Available at: https://doi.org/10.1155/2016/4696803

Zahara, H., Karma, T., Yusuf, M. (2023) 'Klasifikasi daun biduri (*Calotropis gigantea* L.) dari lokasi beberapa menggunakan spektroskopi inframerah dan kemometrik', *Lantanida Journal*, 11(2), pp. 107–117. Available at: https://doi.org/10.22373/lj.v11i2.15096

Zhang, S., Kou, X., Zhao, H., Mak, K., Balijepalli, M.K., Pichika, M.R. (2022) '*Zingiber officinale* var. rubrum : Red Ginger's Medicinal Uses', *Molecules*, 27(3), 775. Available at: https://doi.org/10.3390/molecules27030775